[16] A. Glaser and V. Rokhlin, "A new class of highly accurate solver for ordinary differential equations," *J. Sci. Comput.*, vol. 38, no. 3, pp. 368–399, 2009.
[17] H. Cheng, Z. Gimbutas, P. G. Martinsson, and V. Rokhlin, "On the compression of low rank matrices," *SIAM J. Sci. Comput.*, vol. 26, no. 4, pp. 1389–1404, 2005.
[18] M. Gu and S. C. Eisenstat, "Efficient algorithms for computing a strong rank-revealing QR factorization," *SIAM J. Sci. Comput.*, vol. 17, no. 4, pp. 848–869, 1996.
[19] K. Sirenko, V. Pazynin, Y. Sirenko, and H. Bagci, "An FFT-accelerated FDTD scheme with exact absorbing conditions for characterizing axially symmetric resonant structures," *Progress Electromagn. Res.*, vol. 111, pp. 331–364, Jan. 2011.
[20] J. Smajic, C. Hafner, and D. Erni, "Optimization of photonic crystal structures," *J. Opt. Soc. Am. A*, vol. 21, no. 11, pp. 2223–2232, Nov. 2004.

Discrete Geometric Formulation of Admittance Boundary Conditions for Frequency Domain Problems Over Tetrahedral Dual Grids

L. Codecasa, R. Specogna, and F. Trevisan

***Abstract*—In this work, it is shown how admittance boundary conditions for electromagnetic boundary value problems in the frequency domain can be formulated for the Discrete Geometric Approach. The details are presented for primal grids composed of tetrahedra and barycentric dual grids.**

***Index Terms*—Admittance boundary conditions, cell complexes, discrete geometric approach.**

I. Introduction

The geometric structure on which different physical theories are based, and especially electromagnetism with Maxwell's equations, allows to express these equations in a discrete manner with respect to a pair of oriented and interconnected grids, one dual to the other, leading to the so-called discrete geometric approach (DGA) for computational electromagnetics. This idea has a solid physical and mathematical foundation, reflected in the scientific work of Prof. A. Bossavit with the understanding of the geometric properties of the finite element method [1]–[3], the work of Prof. T. Weiland regarding the finite integration technique [4], of Prof. E. Tonti with the cell method [5]–[7] and Prof. F. L. Teixeira about the formulation of the problem with differential forms [8], [9]. We will develop the treatment of admittance boundary condition in the framework of the DGA; such conditions are convenient when equivalent surface impedance models are developed to represent complex electromagnetic media in high frequency applications, such as the absorbers on the walls of anechoic chambers [10].

Manuscript received September 28, 2011; revised December 27, 2011; accepted March 23, 2012. Date of publication May 23, 2012; date of current version July 31, 2012.

L. Codecasa is with the Politecnico di Milano, I-20133 Milan, Italy (e-mail: codecasa@elet.polimi.it).

R. Specogna and F. Trevisan are with the Università di Udine, Via delle Scienze 208, I-33100 Udine, Italy (e-mail: trevisan@uniud.it; pecogna@uniud.it).

Color versions of one or more of the figures in this communication are available online at http://ieeexplore.ieee.org.

Digital Object Identifier 10.1109/TAP.2012.2201110

The fundamental steps of DGA can be summarized as follows. Firstly the region Ω, in which the problem is set, is discretized by means of a primal grid $\mathcal{G}$ and a dual grid $\tilde{\mathcal{G}}$; then the electromagnetic field is discretized over the grids $\mathcal{G}$ and $\tilde{\mathcal{G}}$. Finally, Maxwell's equations and constitutive relations are reformulated into their corresponding discrete algebraic counterparts.

In DGA, however the formulation of boundary conditions is not explicitly introduced, as commonly reported in [4], [7], since the DGA equations implicitly assume either electric or magnetic wall boundary conditions. The novelty content of this work is to show how a more general class of boundary conditions, like the *admittance boundary conditions*, can be taken into account in DGA in a geometric way, by extending the energy approach previously proposed by the Authors focussing on a primal grid based on tetrahedra and a dual grid obtained from the primal by the barycentric subdivision.

A numerical result is presented to demonstrate the accuracy of the proposed formulation.

II. Formulation of the Electromagnetic Problem

A frequency-domain electromagnetic boundary value problem is considered at angular frequency ω in a *bounded* spatial region Ω. The electromagnetic field is described in terms of phasors by the electric field $\mathbf{e}(\mathbf{r})$, the electric displacement $\mathbf{d}(\mathbf{r})$, the magnetic induction $\mathbf{b}(\mathbf{r})$ and the magnetic field $\mathbf{h}(\mathbf{r})$. These complex vectors are functions of the position vector $\mathbf{r} \in \Omega$ and they are respectively ruled by Faraday-Neumann law

$$\nabla \times \mathbf{e}(\mathbf{r}) = -i\omega\mathbf{b}(\mathbf{r}) \tag{1}$$

and Ampère-Maxwell law

$$\nabla \times \mathbf{h}(\mathbf{r}) = i\omega\mathbf{d}(\mathbf{r}) + \mathbf{j}_s(\mathbf{r}) \tag{2}$$

where $\mathbf{j}_s(\mathbf{r})$ is the specified current density source.

Linear, non-dispersive, in general anisotropic electromagnetic media are considered. Thus the *electric* constitutive relation is

$$\mathbf{d}(\mathbf{r}) = \varepsilon(\mathbf{r})\mathbf{e}(\mathbf{r}) \tag{3}$$

in which $\varepsilon(\mathbf{r})$ is the permittivity double tensor, assumed to be symmetric, positive-definite; the *magnetic* constitutive relation is

$$\mathbf{h}(\mathbf{r}) = \boldsymbol{\nu}(\mathbf{r})\mathbf{b}(\mathbf{r}) \tag{4}$$

where $\boldsymbol{\nu}(\mathbf{r})$ is the reluctivity double tensor, again assumed symmetric and positive-definite.

In addition, boundary conditions on $\mathbf{r} \in \partial\Omega$ are considered, in which $\partial\Omega$ is the boundary of Ω. The boundary conditions can be conveniently expressed in terms of *admittance boundary conditions* as

$$(\mathbf{n}(\mathbf{r}) \times \mathbf{h}(\mathbf{r})) \times \mathbf{n}(\mathbf{r}) = Y(\mathbf{r})(\mathbf{n}(\mathbf{r}) \times \mathbf{e}(\mathbf{r})) \tag{5}$$

where $\mathbf{n}(\mathbf{r})$ is the outward unit vector normal to $\partial\Omega$ at point $\mathbf{r}$ and $Y(\mathbf{r})$ is the admittance at the same point; as particular cases, the perfect electric conductor $\mathbf{n}(\mathbf{r}) \times \mathbf{e}(\mathbf{r}) = \mathbf{0}$ or the magnetic wall $\mathbf{n}(\mathbf{r}) \times \mathbf{h}(\mathbf{r}) = \mathbf{0}$ boundary conditions can be considered also.

III. Spatial Discretization of the Electromagnetic Problem

The frequency-domain electromagnetic problem is spatially discretized by DGA as follows. The spatial region Ω is covered by a pair of oriented and interlocked dual grids $\mathcal{G}$, $\tilde{\mathcal{G}}$, Fig. 1. The primal grid

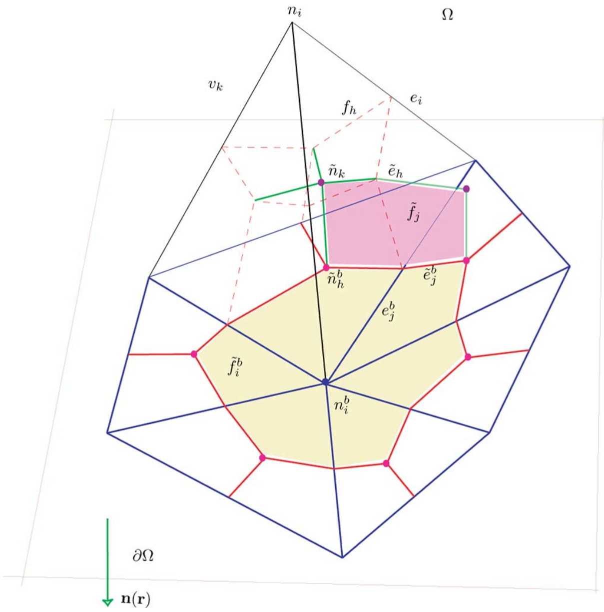

Fig. 1. Some geometric elements of the pair of grids $\mathcal{G}$ and $\tilde{\mathcal{G}}$ are shown, evidencing also the geometric elements on the boundary $\partial\Omega$.

$\mathcal{G}$ is based on simplexes and it consists of a set of nodes $\{n_i\}$, edges $\{e_j\}$, faces (triangles) $\{f_h\}$ and volumes (tetrahedra) $\{v_k\}$; each of these geometrical elements is given an orientation. We denote with $\mathcal{N}$, $\mathcal{E}$, $\mathcal{F}$, $\mathcal{V}$ the cardinalities of each set of geometrical elements, respectively. The dual grid $\tilde{\mathcal{G}}$ is obtained according to the barycentric subdivision of the primal grid $\mathcal{G}$ yielding to the sets of dual volumes $\{\tilde{v}_i\}, i = 1,\ldots,\mathcal{N}$, dual faces $\{\tilde{f}_j\}, j = 1,\ldots,\mathcal{E}$, dual edges, $\{\tilde{e}_h\}$, $h = 1,\ldots,\mathcal{F}$ and dual nodes $\{\tilde{n}_k\}$, $k = 1,\ldots,\mathcal{V}$, respectively. Each geometrical element of $\tilde{\mathcal{G}}$ is in a one-to-one correspondence with and inherits the orientation of the corresponding geometrical element of $\mathcal{G}$. The topologies of $\mathcal{G}$ and $\tilde{\mathcal{G}}$ are described by usual incidence matrices; in our problem, we are interested in the incidence matrix $\mathbf{C}$ between the pairs (f_h, e_j) of dimension $\mathcal{F} \times \mathcal{E}$. In addition, we need the incidence matrix $\tilde{\mathbf{C}}$ between the pairs $(\tilde{f}_j, \tilde{e}_h)$; the following result $\tilde{\mathbf{C}} = \mathbf{C}^T$ holds.

The non empty intersections of each face of $\tilde{\mathcal{G}}$ with the boundary $\partial\Omega$ of the domain define edges $\{\tilde{e}^b_{j_b}\}$, $j_b = 1,\ldots,\mathcal{E}^b$, on the boundary $\partial\Omega$ that can be arbitrarily oriented, Fig. 1; such dual edges pair with the primal edges $\{e^b_j\}$ resulting from the intersection of $\mathcal{G}$ with the boundary $\partial\Omega$, $\mathcal{E}^b$ being the number of the primal edges laying $\partial\Omega$. We also introduce, boundary dual faces $\left\{\tilde{f}^b_{i_b}\right\}$, $i_b = 1,\ldots,\mathcal{N}^b$ on the boundary $\partial\Omega$, Fig. 1, and boundary dual nodes $\{\tilde{n}^b_{h_b}\}$, $h_b = 1,\ldots,\mathcal{F}^b$, where $\mathcal{N}^b$ and $\mathcal{F}^b$ denote the number of primal nodes $\{n^b_i\}$ and primal faces $\{f^b_h\}$ of $\mathcal{G}$ belonging to $\partial\Omega$, respectively. The dual edges $\{\tilde{e}^b_{j_b}\}$ and dual faces $\left\{\tilde{f}^b_{i_b}\right\}$ complete the dual grid $\tilde{\mathcal{G}}$.

The pairs of these edges $\{\tilde{e}^b_{j_b}\}$, $\{e^b_j\}$ with $j_b = 1,\ldots,\mathcal{E}^b$ will allow the geometric formulation of admittance boundary conditions.

Moreover, we evidenced in Fig. 1 a particular type of dual faces $\tilde{f}_j$ whose boundary is formed by dual edges internal to Ω and by only one boundary dual edge $\tilde{e}^b_{j_b(j)}$; $\tilde{e}^b_{j_b(j)}$ is crossed by the primal edge e^b_j and function $j_b(j)$ yields the index corresponding to j, with $j_b = 1,\ldots,\mathcal{E}^b$. We denote with $K_{j_b(j)}$ the incidence number between the pair $(\tilde{f}_j, \tilde{e}^b_{j_b(j)})$.

A. Discretization of the Electromagnetic Field

The electromagnetic field quantities in Section II are discretized in terms of integral quantities associated with the geometric elements of the pair of grids $\mathcal{G}$, $\tilde{\mathcal{G}}$ and the additional edges introduced on the boundary yielding to complex arrays of Degrees of Freedom. On $\mathcal{G}$, we introduce the $\mathcal{E} \times 1$ array $\mathbf{U}$, of voltages $U_j = \int_{e_j} \mathbf{e}(\mathbf{r}) \cdot \mathbf{t}dl$, with $j = 1,\ldots,\mathcal{E}$, along the primal edges $\{e_j\}$ and the $\mathcal{F} \times 1$ array $\mathbf{\Phi}$, of induction fluxes $\Phi_h = \int_{f_h} \mathbf{b}(\mathbf{r}) \cdot \mathbf{n}ds$ with $h = 1,\ldots,\mathcal{F}$ associated with the primal faces $\{f_h\}$; we denoted with $\mathbf{t}$, $\mathbf{n}$ the unit vectors orienting an edge or a face, respectively, both of $\mathcal{G}$ or of $\tilde{\mathcal{G}}$ according to the case.

On $\tilde{\mathcal{G}}$, we introduce the $\mathcal{F} \times 1$ array $\mathbf{F}$ of magneto motive forces; its components $F_h = \int_{\tilde{e}_h} \mathbf{h}(\mathbf{r}) \cdot \mathbf{t}dl$, with $h = 1,\ldots,\mathcal{F}$, are associated with dual edges $\tilde{e}_h \in \tilde{\mathcal{G}}$. On the additional boundary edges we introduce the $\mathcal{E}^b \times 1$ array $\mathbf{F}^b$ of magneto motive forces $F^b_{j_b}$ with $j_b = 1,\ldots,\mathcal{E}^b$ associated with dual edges $\tilde{e}^b_{j_b}$.

Moreover, we introduce the $\mathcal{E} \times 1$ array $\mathbf{\Psi}$, of electric fluxes $\Psi_j = \int_{\tilde{f}_j} \mathbf{d}(\mathbf{r}) \cdot \mathbf{n}ds$ with $j = 1,\ldots,\mathcal{E}$, associated with the dual faces $\{\tilde{f}_j\}$ of $\tilde{\mathcal{G}}$ and the $\mathcal{E} \times 1$ array $\mathbf{I}_s$ of electric currents $I_{sj} = \int_{\tilde{f}_j} \mathbf{j}(\mathbf{r}) \cdot \mathbf{n}ds$, with $j = 1,\ldots,\mathcal{E}$, through the dual faces $\{\tilde{f}_j\}$ of $\tilde{\mathcal{G}}$.

B. Balance Relations

The arrays $\mathbf{U}$, $\mathbf{\Phi}$ are related by the discrete counterpart of (1), formulated in terms of balance equations in a one to one correspondence with each primal face $f_i \in \mathcal{G}$

$$(\mathbf{CU})_i = -i\omega(\mathbf{\Phi})_i, \text{ with } i = 1,\ldots,\mathcal{F} \tag{6}$$

where $(\bullet)_i$ denotes the i-th component of an array. The arrays $\mathbf{\Psi}$, $\mathbf{F}$ are related by the discrete counterpart of (2), formulated in terms of balance equations in a one to one correspondence with a dual face $\tilde{f}_i \in \mathcal{G}$. In the case of a dual face $\tilde{f}_j \in \tilde{\mathcal{G}}$ in a one to one correspondence with a primal edge e_j internal to Ω, we write

$$\left(\mathbf{C}^T\mathbf{F}\right)_j = i\omega(\mathbf{\Psi})_j + (\mathbf{I}_s)_j, \; j = 1,\ldots,\mathcal{E} - \mathcal{E}^b \tag{7}$$

while for a dual face $\tilde{f}_j \in \tilde{\mathcal{G}}$ in a one to one correspondence with a boundary primal edge e^b_j, we write

$$\left(\mathbf{C}^T\mathbf{F}\right)_j + K_{j_b(j)}(\mathbf{F}^b)_{j_b(j)} = i\omega(\mathbf{\Psi})_j + (\mathbf{I}_s)_j \tag{8}$$

with $j = \mathcal{E} - \mathcal{E}^b + 1,\ldots,\mathcal{E}$, where $(\mathbf{F}^b)_{j_b(j)}$ is the m.m.f. associated with the only one dual boundary edge $\tilde{e}^b_j$ belonging to $\partial\tilde{f}_j$ and function $j_b(j)$ yields the component of $\mathbf{F}^b$ corresponding to j.

C. Discrete Counterparts of Constitutive Relations

The *electric* constitutive relation (3) is discretized into the matrix equation

$$\mathbf{\Psi} = \mathbf{EU} \tag{9}$$

in which the $\mathcal{E} \times \mathcal{E}$ matrix $\mathbf{E}$ is a discrete counterpart of the $\boldsymbol{\varepsilon}(\boldsymbol{r})$ tensor. The *magnetic* constitutive relation (4) is discretized into the matrix equation

$$\mathbf{F} = \mathbf{M\Phi} \tag{10}$$

in which the $\mathcal{F} \times \mathcal{F}$ matrix $\mathbf{M}$ is a discrete counterpart of the $\boldsymbol{\nu}(\boldsymbol{r})$ tensor. The problem of discretizing constitutive relations is crucial in DGA; in order to guarantee stability and consistency of the overall discretized electromagnetic problem, the matrices $\mathbf{E}$, $\mathbf{M}$ are required to be symmetric positive definite and consistent[1]. To construct the constitutive matrices the edge and face vector base functions defined in [11], [12] and [13] can be used. These vector base functions assure

[1]A precise definition of the notion of consistency for constitutive matrices is given in [3].

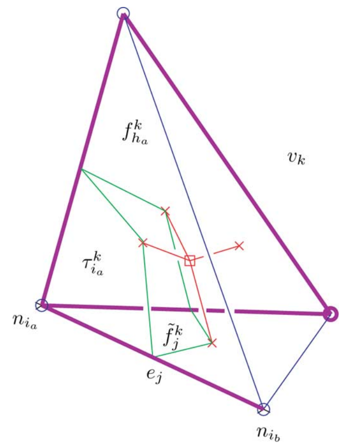

Fig. 2. Primal volume v_k of the cluster of tetrahedra around a primal edge e_j is shown together with the portion of dual volume $\tau_{i_a}^k$ tailored inside v_k and in a one to one correspondence with n_{i_a}. Moreover the restriction of the dual face $\tilde{f}_j^k$ is drawn. The pair formed by the face $f_{h_a}^k$ and edge e_j having the node n_{i_a} in common is evidenced.

that symmetry, positive-definiteness, and consistency of the constitutive matrices are guaranteed.

D. Discrete Counterpart of Admittance Boundary Conditions

We will demonstrate how admittance boundary conditions (5) can be discretized on the pair of boundary grids $\mathcal{G}^b$, $\tilde{\mathcal{G}}^b$ as

$$\mathbf{F}^b = \mathbf{Y}\mathbf{U}^b \tag{11}$$

where $\mathbf{Y}$ is a square $\mathcal{E}^b \times \mathcal{E}^b$ symmetric positive definite matrix representing a discrete counterpart of the admittance $Y(\boldsymbol{r})$; the array $\mathbf{U}^b$ is a subarray of the array $\mathbf{U}$, having as entries the voltages $U_{j_b}^b$ associated with the boundary primal edges $e_{j_b}^b$, with $j_b = 1, \ldots, \mathcal{E}^b$.

IV. Discrete Electromagnetic Field Problem

Now, we can state the electromagnetic problem spatially discretized, with respect to the pair of grids $\mathcal{G}$, $\tilde{\mathcal{G}}$ in Ω as follows: *solve* (6)–(10) *subject to discrete admittance boundary conditions* (11)*, by computing the complex arrays* $\mathbf{U}$, $\mathbf{\Phi}$, $\mathbf{F}$, $\mathbf{\Psi}$, $\mathbf{F}^b$ *for the angular frequency* ω. The constitutive matrices $\mathbf{M}$ and $\mathbf{E}$ proposed in [11], [13] guarantee convergence of the discrete electromagnetic problem under mild regularity conditions on the electromagnetic problem and on the pair of dual grids [14] in the hypothesis of either perfect electric boundary condition (PEC) or perfect magnetic boundary conditions (PMC).

It is convenient to reformulate the discrete electromagnetic field problem in terms of the array $\mathbf{U}$, by substituting in (7)–(9) for $\mathbf{\Psi}$, (10) for $\mathbf{F}$; we write

$$(\mathbf{C}^T\mathbf{M}\mathbf{\Phi})_j = i\omega(\mathbf{E}\mathbf{U})_j + (\mathbf{I}_s)_j \quad j = 1, \ldots, \mathcal{E} - \mathcal{E}^b \tag{12}$$

$$(\mathbf{C}^T\mathbf{M}\mathbf{\Phi})_j + K_{j_b(j)}(\mathbf{F}^b)_{j_b(j)} = i\omega(\mathbf{E}\mathbf{U})_j + (\mathbf{I}_s)_j \tag{13}$$

with $j = \mathcal{E} - \mathcal{E}^b + 1, \ldots, \mathcal{E}$ in this last equation. Next, deducing $\mathbf{\Phi}$ from (6) and substituting in (12) and (13) we obtain respectively

$$((\mathbf{C}^T\mathbf{M}\mathbf{C} - \omega^2\mathbf{E})\mathbf{U})_j = -i\omega(\mathbf{I}_s)_j \quad j = 1, \ldots, \mathcal{E} - \mathcal{E}^b \tag{14}$$

and using (11) for $\mathbf{F}^b$, (13) yields

$$((\mathbf{C}^T\mathbf{M}\mathbf{C} - \omega^2\mathbf{E})\mathbf{U})_j - i\omega K_{j_b(j)}(\mathbf{Y}\mathbf{U}^b)_{j_b(j)} = -i\omega(\mathbf{I}_s)_j \tag{15}$$

with $j = \mathcal{E} - \mathcal{E}^b + 1, \ldots, \mathcal{E}$.

In this communication, we will focus on the computation of matrix $\mathbf{Y}$; in preparation of the computation of $\mathbf{Y}$ the computation of $\mathbf{E}$ is revisited.

V. Constitutive Matrix E

In order to build the matrix $\mathbf{E}$, we use a set of piece-wise uniform edge vector functions and an energy approach introduced in [12], [13].

We focus on a primal edge $e_j \in \mathcal{G}$, with $j = 1, \ldots, \mathcal{E}$, whose boundary nodes are n_{i_a}, n_{i_b}, with $i_a, i_b \in \{1, \ldots, \mathcal{N}\}$ and we consider a tetrahedron v_k of the cluster $\mathcal{C}_j$ of tetrahedra around e_j.

The dual volumes corresponding to n_{i_a}, n_{i_b} are denoted with $\tilde{v}_{i_a}$, $\tilde{v}_{i_b}$ respectively. The intersection between $\tilde{v}_{i_a}$ and v_k is $\tau_{i_a}^k$, Fig. 2; similarly, $\tau_{i_b}^k$ is the intersection between $\tilde{v}_{i_b}$ and v_k.

We denote with $f_{h_a}^k$, $f_{h_b}^k$ the pair of primal faces of v_k opposite to the edge e_j and having the nodes n_{i_a}, n_{i_b} in common with e_j, respectively. Correspondingly, $\mathbf{f}_{h_a}^k$, $\mathbf{f}_{h_b}^k$ denote the face vectors associated with $f_{h_a}^k$, $f_{h_b}^k$; a face vector is a vector normal to the face, pointing *outward* with respect to the volume v_k and with amplitude equal to the area of the face.

The union set $\cup_{k=1}^{\mathrm{card}(\mathcal{C}_j)} \tau_{i_a}^k \cup \tau_{i_b}^k = \tau_j$ is the support of the edge vector function $\mathbf{v}_j^e(\mathbf{r})$ attached to e_j, defined as

$$\mathbf{v}_j^e(\mathbf{r}) = \begin{cases} G_{ji_a}\dfrac{\mathbf{f}_{h_a}^k}{3|v_k|}, & \text{if } \mathbf{r} \in \tau_{i_a}^k \\ G_{ji_b}\dfrac{\mathbf{f}_{h_b}^k}{3|v_k|}, & \text{if } \mathbf{r} \in \tau_{i_b}^k \end{cases} \tag{16}$$

where G_{ji_a}, G_{ji_b} are the incidence numbers between the pairs (e_j, n_{i_a}) and (e_j, n_{i_b}), respectively[2]; $|v_k|$ is the volume of the tetrahedron v_k.

As proved in [12], [13], $\mathbf{v}_j^e(\mathbf{r})$ form a base and they can represent *exactly* an element wise uniform electric field from the voltages on primal edges as

$$\mathbf{e}(\mathbf{r}) = \sum_{j=1}^{\mathcal{E}} \mathbf{v}_j^e(\mathbf{r})U_j. \tag{17}$$

Moreover, the entries of a symmetric positive definite and consistent matrix $\mathbf{E}$, can be computed as

$$(\mathbf{E})_{ij} = \int_\Omega \mathbf{v}_i^e \cdot \varepsilon\mathbf{v}_j^e dv. \tag{18}$$

VI. Tangent Electric Field on $\partial\Omega$

From (17) and the definition (16) of edge vector functions, the component of the electric field $\mathbf{e}(\mathbf{r})$ tangent to $\partial\Omega$, with $\mathbf{r} \in \partial\Omega$, can be represented as

$$(\mathbf{n}(\mathbf{r}) \times \mathbf{e}(\mathbf{r})) \times \mathbf{n}(\mathbf{r}) = \sum_{j=1}^{\mathcal{E}} \left(\mathbf{n}(\mathbf{r}) \times \mathbf{v}_j^e(\mathbf{r})\right) \times \mathbf{n}(\mathbf{r})U_j = \tag{19}$$

$$= \sum_{j=1}^{\mathcal{E}^b} \mathbf{v}_j^{eb}(\mathbf{r})U_j^b \tag{20}$$

[2]A primal node is always oriented as a sink.

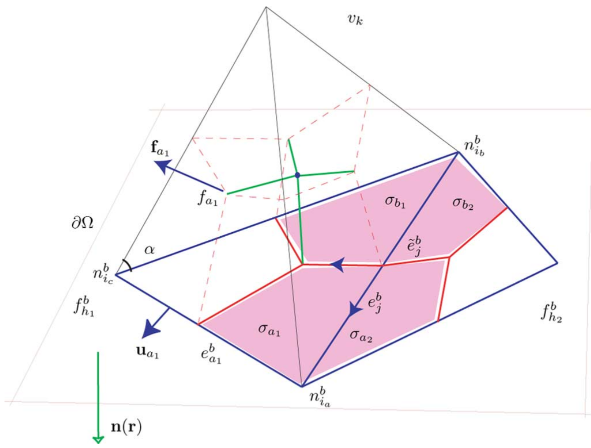

Fig. 3. A portion of the $\partial\Omega$ oriented by the normal $\mathbf{n}(\mathbf{r})$ is shown with a number of geometric elements on the boundary $\partial\Omega$. In particular, the support σ^b_j of the boundary edge vector function $\mathbf{v}^{eb}_j(\mathbf{r})$ and the unit vector $\mathbf{u}_{a_1}$ are evidenced.

where $\mathbf{n}(\mathbf{r})$ is the outward unit vector normal to $\partial\Omega$ and $\mathbf{v}^{eb}_j(\mathbf{r})$ is the j-th edge vector function associated with a boundary edge e^b_j defined as

$$\mathbf{v}^{eb}_j(\mathbf{r}) = \big(\mathbf{n}(\mathbf{r}) \times \mathbf{v}^e_j(\mathbf{r})\big) \times \mathbf{n}(\mathbf{r}). \tag{21}$$

The support σ^b_j of $\mathbf{v}^{eb}_j(\mathbf{r})$ attached to e^b_j follows from the definition of the support of edge vector functions (16). We denote with n^b_{ia}, n^b_{ib} the boundary nodes of e^b_j and with $\tilde{f}^b_{i_a}$, $\tilde{f}^b_{i_b}$ the corresponding pair of boundary dual faces; moreover, $f^b_{h_1}$, $f^b_{h_2}$ is the pair of boundary primal faces adjacent to e^b_j. Introducing the intersections $\sigma_{a_1} = \tilde{f}^b_{i_a} \cap f^b_{h_1}$, $\sigma_{b_1} = \tilde{f}^b_{i_b} \cap f^b_{h_1}$, $\sigma_{a_2} = \tilde{f}^b_{i_a} \cap f^b_{h_2}$, $\sigma_{b_2} = \tilde{f}^b_{i_b} \cap f^b_{h_2}$ then we have that $\sigma^b_j = (\sigma_{a_1} \cup \sigma_{a_2}) \cup (\sigma_{b_1} \cup \sigma_{b_2})$ holds, Fig. 3.

From (21), we will deduce the corresponding geometric representation of $\mathbf{v}^{eb}_j(\mathbf{r})$. With reference to Fig. 3 and assuming $\mathbf{r} \in \sigma_{a_1}$, from (16) we may write

$$\mathbf{n}(\mathbf{r}) \times \mathbf{v}^e_j(\mathbf{r}) = G_{ji_a}\mathbf{n}(\mathbf{r}) \times \frac{\mathbf{f}_{a_1}}{3|v_k|} = \tag{22}$$

$$= G_{ji_a}\frac{-G_{a_1 i_a}\mathbf{e}^b_{a_1}}{|\mathbf{e}^b_{a_1}|}\frac{|\mathbf{f}_{a_1}|}{3|v_k|}\sin\alpha = -G_{ji_a}\frac{G_{a_1 i_a}\mathbf{e}^b_{a_1}}{2|f^b_{h_1}|} \tag{23}$$

where $G_{a_1 i_a}$ is the incidence number between the boundary edge $e^b_{a_1}$ of $f^b_{h_1}$, drawn from the node $n^b_{i_a}$ and the edge $e^b_{a_1}$, Fig. 3; $\mathbf{e}^b_{a_1}$ is the edge vector associated with and oriented as the edge $e^b_{a_1}$, α is the angle between the faces f_{a_1} and $f^b_{h_1}$; note that the vector $G_{a_1 i_a}\mathbf{e}^b_{a_1}$ always points towards $n^b_{i_a}$. The last equality in (23) stems from elementary geometry since $|f_{a_1}| = \left|e^b_{a_1}\right| h/2$, h being the height of the triangle f_{a_1} with respect to $e^b_{a_1}$ and $|v_k| = \left|f^b_{h_1}\right| H/3$, H being the height of the tetrahedron v_k with respect to $f^b_{h_1}$. From (23), we deduce

$$\big(\mathbf{n}(\mathbf{r}) \times \mathbf{v}^e_j(\mathbf{r})\big) \times \mathbf{n}(\mathbf{r}) = G_{ji_a}\frac{\mathbf{u}_{a_1}}{d_{a_1}} \tag{24}$$

where $d_{a_1} = \left|\mathbf{e}^b_{a_1}\right|/2\left|f^b_{h_1}\right|$ is the height the triangle $f^b_{h_1}$ with respect to $e^b_{a_1}$, and $\mathbf{u}_{a_1}$ is the unit vector normal to $e^b_{a_1}$ on $\partial\Omega$ pointing *outward* $f^b_{h_1}$.

Therefore, the boundary edge vector function $\mathbf{v}^{eb}_j(\mathbf{r})$ attached to e^b_j of support σ_j is defined as

$$\mathbf{v}^{eb}_j(\mathbf{r}) = \begin{cases} G_{ji_a}\frac{\mathbf{u}_{a_s}}{d_{a_s}}, & \text{if } \mathbf{r} \in \sigma_{a_s} \\ G_{ji_b}\frac{\mathbf{u}_{b_s}}{d_{b_s}}, & \text{if } \mathbf{r} \in \sigma_{b_s} \end{cases} \tag{25}$$

where for $\mathbf{r} \in \sigma_{a_s}$, $d_{a_s} = \left|\mathbf{e}^b_{a_s}\right|/2\left|f^b_{h_s}\right|$ is the height the triangle $f^b_{h_s}$ with respect to $e^b_{a_s}$, and $\mathbf{u}_{a_s}$ is the unit vector normal to $e^b_{a_s}$ on $\partial\Omega$ pointing outward $f^b_{h_s}$, with the index $s = 1, 2$; similarly for $\mathbf{r} \in \sigma_{b_s}$.

The set of boundary edge vector functions $\left\{\mathbf{v}^{eb}_j(\mathbf{r})\right\}$ form a basis, since from elementary geometry $\int_{e^b_i}\mathbf{v}^{eb}_j(\mathbf{r}) \cdot \mathbf{t}dl = \delta_{ij}$ holds for i, $j = 1, \ldots, \mathcal{E}^b$, δ_{ij} being the Kronecker symbol and $\mathbf{t}$ the unit tangent vector to e^b_i.

A. Geometric Property of $\mathbf{v}^{eb}_j(\mathbf{r})$

We will now demonstrate a geometric property fundamental to construct the constitutive matrix (11).

Theorem 1: The boundary edge vector function $\mathbf{v}^{eb}_j(\mathbf{r})$ satisfies the following consistency condition

$$\int_{f^b_h}\mathbf{v}^{eb}_j(\mathbf{r})ds = \int_{f^b_h \cap \tilde{e}^b_j}\mathbf{t}(\mathbf{r}) \times \mathbf{n}(\mathbf{r})dl \tag{26}$$

in which f^b_h is the h-th face of $\mathcal{G}^b$ and $\tilde{e}^b_j$ is the j-th dual edge of $\tilde{\mathcal{G}}^b$ of unit tangent vector $\mathbf{t}(\mathbf{r})$.

Proof: For the triangle $f^b_{h_1}$ shown in Fig. 3 of vertices $n^b_{i_a}$, $n^b_{i_b}$, $n^b_{i_c}$, without loosing generality, we assume the edge e^b_j oriented from $n^b_{i_b}$ to $n^b_{i_a}$; with $\mathbf{r} \in \sigma_{a_1}$ (25) yields $\mathbf{v}^{eb}_j(\mathbf{r}) = (\mathbf{r}_{i_c} - \mathbf{r}_{i_a}) \times \mathbf{n}/2\left|f^b_{h_1}\right|$; with $\mathbf{r} \in \sigma_{b_1}$ (25) yields $\mathbf{v}^{eb}_j(\mathbf{r}) = (\mathbf{r}_{i_c} - \mathbf{r}_{i_b}) \times \mathbf{n}/2\left|f^b_{h_1}\right|$ since $G_{ji_a} = -G_{ji_b} = +1$. Thence

$$\begin{aligned}\int_{f^b_{h_1}}\mathbf{v}^{eb}_j(\mathbf{r})ds &= \frac{(\mathbf{r}_{i_c} - \mathbf{r}_{i_a}) \times \mathbf{n}}{2\left|f^b_{h_1}\right|}\frac{\left|f^b_{h_1}\right|}{3} + \\ &+ \frac{(\mathbf{r}_{i_c} - \mathbf{r}_{i_b}) \times \mathbf{n}}{2\left|f^b_{h_1}\right|}\frac{\left|f^b_{h_1}\right|}{3} \\ &= \frac{\mathbf{r}_{i_c} - \frac{\mathbf{r}_{i_a} + \mathbf{r}_{i_b}}{2}}{3} \times \mathbf{n} \\ &= \int_{f^b_{h_1} \cap \tilde{e}^b_j}\mathbf{t}(\mathbf{r}) \times \mathbf{n}(\mathbf{r})dl,\end{aligned}$$

in which $\mathbf{n}$ is the unit vector normal to $f^b_{h_1}$ pointing outward Ω and $\mathbf{t}$ is the unit vector tangent to $f^b_{h_1} \cap \tilde{e}^b_j$ congruent with the orientation[3] of the dual edge $\tilde{e}^b_j$. ∎

As a corollary, we have that

$$\int_{f^b_h}\left(\mathbf{n}(\mathbf{r}) \times \mathbf{v}^{eb}_j(\mathbf{r})\right)ds = \int_{f^b_h \cap \tilde{e}^b_j}\mathbf{t}(\mathbf{r})dl \tag{27}$$

holds. Dot multiplying (27) by the uniform field $(\mathbf{n}(\mathbf{r}) \times \mathbf{h}(\mathbf{r})) \times \mathbf{n}(\mathbf{r})$ in f^b_h, we obtain

$$\int_{f^b_h}\left(\mathbf{n}(\mathbf{r}) \times \mathbf{v}^{eb}_j(\mathbf{r})\right) \cdot \mathbf{h}(\mathbf{r})ds = \int_{f^b_h \cap \tilde{e}^b_j}\mathbf{h}(\mathbf{r}) \cdot \mathbf{t}(\mathbf{r})dl. \tag{28}$$

VII. Constitutive Matrix $\mathbf{Y}$

As a first step, we will apply the energy approach [12], [13] specifically tailored for a pair of independent fields $\mathbf{e}(\mathbf{r})'$, $\mathbf{h}(\mathbf{r})$; in terms of their tangent components on $\partial\Omega$, we write $(\mathbf{n}(\mathbf{r}) \times \mathbf{e}(\mathbf{r})') \times \mathbf{n}(\mathbf{r})$ and $\mathbf{n}(\mathbf{r}) \times \mathbf{h}(\mathbf{r})$ respectively. Then (5) yields

$$\mathbf{h}(\mathbf{r}) \times \mathbf{n}(\mathbf{r}) = Y(\mathbf{r})(\mathbf{n}(\mathbf{r}) \times \mathbf{e}(\mathbf{r})) \times \mathbf{n}(\mathbf{r}) \tag{29}$$

where $\mathbf{e}(\mathbf{r})$ is kept distinct from $\mathbf{e}(\mathbf{r})'$.

We compute the flux of the vector $\mathbf{e}(\mathbf{r})' \times \mathbf{h}(\mathbf{r})^*$ and we use (20) for $(\mathbf{n}(\mathbf{r}) \times \mathbf{e}(\mathbf{r})') \times \mathbf{n}(\mathbf{r}) = \sum_{j=1}^{\mathcal{E}^b} U^{b\prime}_j\mathbf{v}^{eb}_j(\mathbf{r}), \forall\, U^{b\prime}_j$

[3]An orientation of $\tilde{e}^b_j$ congruent with the orientation of e^b_j can be established in such a way that for the corresponding edge vectors $\mathbf{n} \times \mathbf{e}^b_j \cdot \tilde{\mathbf{e}}^b_j > 0$ holds.

$$
\begin{aligned}
&\int_{\partial\Omega} \mathbf{e}(\mathbf{r})' \times \mathbf{h}(\mathbf{r})^* \cdot \mathbf{n} ds = \\
&= \int_{\partial\Omega} (\mathbf{h}(\mathbf{r}) \times \mathbf{n}(\mathbf{r}))^* \cdot ((\mathbf{n}(\mathbf{r}) \times \mathbf{e}(\mathbf{r})') \times \mathbf{n}(\mathbf{r})) ds = \\
&= \sum_{j=1}^{\mathcal{E}^b} U_j^{b'} \int_{\partial\Omega} (\mathbf{h}(\mathbf{r}) \times \mathbf{n}(\mathbf{r}))^* \cdot \mathbf{v}_j^{eb}(\mathbf{r}) ds = \qquad (30)\\
&= \sum_{j=1}^{\mathcal{E}^b} U_j^{b'} \left(\int_{\partial\Omega} \left(\mathbf{n}(\mathbf{r}) \times \mathbf{v}_j^{eb}(\mathbf{r}) \right) \cdot \mathbf{h}(\mathbf{r}) ds \right)^* = \\
&= \sum_{j=1}^{\mathcal{E}^b} U_j'^b \sum_{h=1}^{\mathcal{F}^b} \left(\int_{f_h^b} \left(\mathbf{n}(\mathbf{r}) \times \mathbf{v}_j^{eb}(\mathbf{r}) \right) \cdot \mathbf{h}(\mathbf{r}) ds \right)^* \qquad (31)
\end{aligned}
$$

and substituting (28) in (31) we obtain that

$$
\begin{aligned}
\int_{\partial\Omega} \mathbf{e}(\mathbf{r})' \times \mathbf{h}(\mathbf{r})^* \cdot \mathbf{n} ds &= \sum_{j=1}^{\mathcal{E}^b} U_j'^b F_j^{b*} \\
&= \mathbf{U}^{b'T} \mathbf{F}^{b*} \qquad (32)
\end{aligned}
$$

holds $\forall\, U_j^{b'}$.

Now, as a second step, by substituting (29) and (20) in (30), we obtain

$$
\begin{aligned}
&\int_{\partial\Omega} \mathbf{e}(\mathbf{r})' \times \mathbf{h}(\mathbf{r})^* \cdot \mathbf{n} ds = \\
&= \int_{\partial\Omega} \left(Y(\mathbf{r}) \sum_{i=1}^{\mathcal{E}^b} U_i^b \mathbf{v}_i^{eb}(\mathbf{r}) \right)^* \cdot \sum_{j=1}^{\mathcal{E}^b} U_j^{b'} \mathbf{v}_j^{eb}(\mathbf{r}) ds = \\
&= \sum_{i,j=1}^{\mathcal{E}^b} U_i^{b*} \left(\int_{\partial\Omega} Y(\mathbf{r}) \mathbf{v}_i^{eb}(\mathbf{r}) \cdot \mathbf{v}_j^{eb}(\mathbf{r}) ds \right)^* U_j^{b'} = \\
&= \mathbf{U}^{b'T} (\mathbf{Y}\mathbf{U}^b)^*. \qquad (33)
\end{aligned}
$$

Since (33) and (31) hold $\forall\, U_j^{b'}$ then $\mathbf{F}^b = \mathbf{Y}\mathbf{U}^b$ holds exactly, where the entry of the matrix $\mathbf{Y}$ is

$$
(\mathbf{Y})_{ij} = \int_{\partial\Omega} Y(\mathbf{r}) \mathbf{v}_i^{eb}(\mathbf{r}) \cdot \mathbf{v}_j^{eb}(\mathbf{r}) ds \qquad (34)
$$

with $i,\, j = 1, \ldots, \mathcal{E}^b$. Matrix $\mathbf{Y}$ is obviously symmetric and since $\left\{ \mathbf{v}_i^{eb}(\mathbf{r}) \right\}$ form a base, $\mathbf{Y}$ is also positive definite; moreover, as we saw, $\mathbf{Y}$ satisfies (11) exactly when the tangent component of the electric field is piece-wise uniform within each primal boundary face of $\mathcal{G}^b$.

Equation (33) relates matrix $\mathbf{Y}$ to the flux of Poynting's vector across the boundary $\partial\Omega$. In this way matrix $\mathbf{Y}$, similarly to matrices $\mathbf{E}$ and $\mathbf{M}$, is determined by an energy approach.

VIII. Numerical Results

The field along a matched section of a square waveguide under TE_{10} excitation has been computed as a test case, being available the analytical solution. The waveguide dimensions are: width a, height $b = a$, length $l = 2a$. The numerical analysis has been performed adopting a uniform mesh composed of tetrahedra.

The percent error of the energy norm of computed electric field, at normalized frequency $f/f_c = 1.5$, is plotted in Fig. 4 for finer and finer grids of maximum diameter h. The error behavior has been compared with $O(h^2)$.

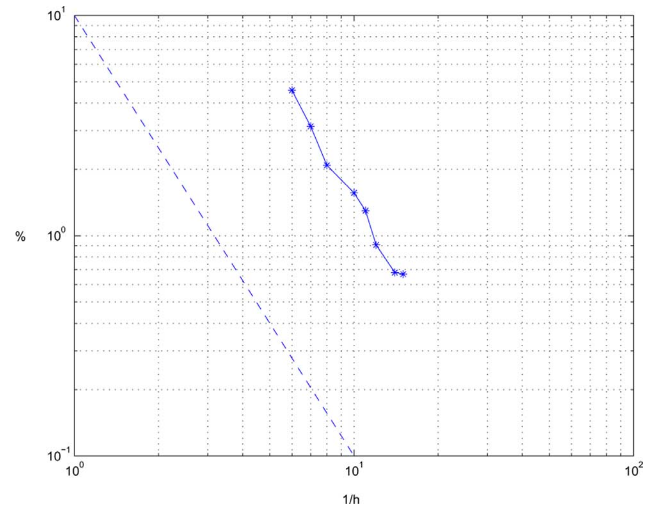

Fig. 4. Percent error at $f/f_c = 1.5$ as a function of h.

IX. Conclusion

In this communication, admittance boundary conditions for the solution by DGA of electromagnetic boundary value problems in the frequency domain, have been formulated using augmented dual grids. The derivation has been carried out for barycentric dual grids.

References

[1] Bossavit, "How weak is the weak solution in finite elements methods?," *IEEE Trans. Magn.*, vol. 34, no. 5, pp. 2429–2432, 1998.

[2] T. Tarhasaari, L. Kettunen, and A. Bossavit, "Some realizations of a discrete Hodge operator: A reinterpretation of finite element techniques," *IEEE Trans. Magn.*, vol. 35, no. 3, pp. 1494–1497, 1999.

[3] A. Bossavit and L. Kettunen, "Yee-like schemes on staggered cellular grids: A synthesis between FIT and FEM approaches," *IEEE Trans. Magn.*, vol. 36, no. 4, pp. 861–867, 2000.

[4] T. Weiland, "A discretization method for the solution of Maxwell's equations for six-component fields," *Electron. Commun. (AEÜ)*, vol. 31, pp. 116–116, 1977.

[5] E. Tonti, "On the Geometrical Structure of Electromagnetism," in *Gravitation, Electromagnetism and Geometrical Structures for the 80th Birthday of A. Lichnerowicz*, G. Ferrarese, Ed. Bologna, Italy: Pitagora Editrice, 1995, pp. 281–308.

[6] E. Tonti, "Algebraic topology and computational electromagnetism," in *Proc. 4th Int. Workshop on Electric and Magnetic Fields*, Marseille (Fr), May 12–15, 1998, pp. 284–294.

[7] E. Tonti, "Finite formulation of the electromagnetic field," *IEEE Trans. Magn.*, vol. 38, no. 2, pp. 333–336, 2002.

[8] F. L. Teixeira and W. C. Chew, "Lattice electromagnetic theory from a topological viewpoint," *J. Math. Phys.*, vol. 40, no. 1, pp. 169–187, 1999.

[9] F. L. Teixeira, "Geometric aspects of the simplicial discretization of Maxwell's equations," *Progr. Electromagn. Res.*, vol. 32, pp. 171–188, 2001.

[10] B. K. Chung and H. T. Chuah, "Design and construction of a multipurpose wideband anechoic chamber," *IEEE Trans. Antennas Propag.*, vol. 45, no. 6, 2003.

[11] L. Codecasa, V. Minerva, and M. Politi, "Use of barycentric dual grids for the solution of frequency domain problems by FIT," *IEEE Trans. Magn.*, vol. 40, no. 2, pp. 1414–1419, 2004.

[12] L. Codecasa and F. Trevisan, "Piecewise uniform bases and energetic approach for discrete constitutive matrices in electromagnetic problems," *Int. J. Numer. Meth. Eng.*, vol. 65, no. 4, pp. 548–565, 2006.

[13] L. Codecasa, R. Specogna, and F. Trevisan, "Symmetric positive-definite constitutive matrices for discrete eddy-current problems," *IEEE Trans. Magn.*, vol. 42, no. 2, pp. 510–515, 2007.

[14] L. Codecasa and F. Trevisan, "Convergence of electromagnetic problems modelled by discrete geometric approach," *CMES*, vol. 58, no. 1, pp. 15–44, 2010.